Research article

Preparation and evaluation of the anti-cancer properties of RGD-modified curcumin-loaded chitosan/perfluorohexane nanocapsules *in vitro*

Liang Wang [a,b], Shixia Zhu [c], Chunpeng Zou [b], Hongju Kou [b], Maosheng Xu [b], Jie Li [a,*]

[a] *Department of Ultrasound, Qilu Hospital of Shandong University, Jinan 250012, China*
[b] *Department of Ultrasound, The Second Affiliated Hospital and Yuying Children's Hospital of Wenzhou Medical University, Wenzhou 325027, China*
[c] *Department of Ultrasound, Wenzhou Seventh People's Hospital, Wenzhou 325005, China*

ARTICLE INFO

ABSTRACT

Curcumin (Cur) encapsulation in nanocapsules (NCs) could improve its availability and therapeutic antitumor efficacy. Cur-loaded chitosan/perfluorohexane (CS/PFH) nanocapsules (CS/PFH-Cur-NCs) were thus synthesized via a nanoemulsion process. To further enhance the selective tumor targeting ability of Cur-loaded NCs, a novel CS/PFH-Cur-NCs with conjugation of Arg-Gly-Asp (RGD) peptide (RGD-CS/PFH-Cur-NCs) were prepared in this study. The properties of these NCs were then explored through *in vitro* release experiments and confocal laser scanning microscopy-based analyses of the ability of these NCs to target MDA-MB-231 breast cancer cells. In addition, an MTT assay-based approach was used to compare the relative cytotoxic impact of CS/PFH-Cur-NCs and RGD-CS/PFH-Cur-NCs on these breast cancer cells. It was found that both CS/PFH-Cur-NCs and RGD-CS/PFH-Cur-NCs were smooth, relatively uniform, spheroid particles, with the latter being 531.20 ± 68.97 nm in size. These RGD-CS/PFH-Cur-NCs can be ideal for contrast imaging studies, and were better able to target breast cancer cells in comparison to CS/PFH-Cur-NCs. In addition, RGD-CS/PFH-Cur-NCs were observed to induce cytotoxic MDA-MB-231 cell death more swiftly in comparison to CS/PFH-Cur-NCs. These findings suggest that NC encapsulation and RGD surface modification can remarkably improve the anti-tumor efficacy of Cur. These novel NCs may thus manifest a significant potential value in the realm of image-guided cancer therapy, underscoring an important direction for future research.

1. Introduction

Curcumin (Cur) is a polyphenol that can be isolated from samples of turmeric root [1]. Prior research has demonstrated that Cur possesses a range of anti-tumor [2, 3], anti-cancer [4, 5], anti-inflammatory [6], antioxidant [7], and anti-ischemic [8] pharmacological properties. In the context of tumor treatment, Cur has been shown to be capable of inducing apoptotic tumor cell death inhibiting the proliferative and invasive activity of these cells [9, 10, 11, 12]. Importantly, Cur is broadly active against a range of tumor types and exhibits synergy with other anti-tumor compounds [13, 14]. However, Cur is a lipophilic compound that therefore exhibits poor solubility, thus hampering its bioavailability and therapeutic efficacy [15, 16, 17]. To overcome these bioavailability limitations, very high Cur doses are required to achieve pharmacological efficacy, thus constraining the degree to which is can be administered in clinical settings [18]. Thus, there is a clear need for the development of a novel drug delivery system capable of improving Cur stability, solubility, and therapeutic efficacy to tumor treatment.

Nanocapsules (NCs) are a commonly studied drug carrier, offering several advantages including the ability to facilitate sustained drug release, thereby prolonging the duration of drug activity and improving overall treatment efficacy [19, 20, 21], leading to widespread interest in the clinical development of such NCs [22, 23, 24, 25]. Chitosan-based polymers are promising nanocarriers for Cur delivery for theranostic applications [26]. Encapsulating Cur in Chitosan/perfluorohexane NCs (CS/PFH-Cur-NCs) could improve its stability and anti-cancer efficacy [27].

However, CS/PFH-Cur-NCs are passive targeting NCs, which lack selectively targeting ability to tumor cells. The Arg-Gly-Asp (RGD) peptide is capable of binding to the αvβ3 and αvβ5 integrins found on the surface of many tumor cells [28]. In previous studies, RGD peptide conjugation has been shown to bolster the anti-tumor efficacy of specific drugs and to improve the targeting of imaging compounds to tumor cells

---

[29, 30]. Suppose CS/PFH-Cur-NCs with conjugation of RGD could better facilitate selectively targeted tumor treatment. Therefore, to further enhance the active targeting ability of NCs to tumor cells, a novel RGD-modified CS/PFH-Cur-NCs (RGD-CS/PFH-Cur-NCs) were prepared. As such, the aim of the present study was to synthesize RGD-CS/PFH-Cur-NCs, and evaluate its selective anti-cancer properties *in vitro*.

2. Materials and methods

2.1. Materials

Curcumin, lecithin, PBS (pH 7.4), Dulbecco's modified Eagle's medium (DMEM), 0.25% trypsin-EDTA, heat-inactivated FBS, and Dimethyl sulfoxide (DMSO) were purchased from Solarbio Life Sciences (Beijing, China). Chitosan (CS), perfluorohexane (PFH), Tween 20, Sephadex G-50, and dialysis membranes (MWCO: 12,000) were purchased from Muke Biotech (Zhejiang, China). Rhodamine *B waspurchased* from Sangon Biotech (Shanghai, China). Arg-Gly-Asp-l-Phe-Lys (RGDfk), N-hydroxysulfosuccinimide (sulfo-NHS), N-(3-dimethylaminopropyl)-N′-ethylcarbodiimide hydrochloride (EDC-HCl), and 3-(4,5)-dimethylthiahiazo (-z-y1)-3,5-di-phenytetrazolium-romide (MTT) were from Sigma-Aldrich (MO, USA). Other chemicals and solvents were obtained commercially of high-performance liquid chromatography (HPLC) or analytical grade. MDA-MB-231 breast cancer cells were from the Cell Bank of the Chinese Academy of Sciences in Shanghai.

2.2. RGD-CS/PFH-cur-NC preparation

A nano-emulsion approach was used to prepare CS/PFH-Cur-NCs, as reported in prior studies [27]. To state briefly, lecithin (3 mg) and Cur (400 mg) in 98% ethanol (100 mL) were homogenized for 3 min in PFH (90 mL) and distilled deionized H_2O (3 mL) at 24,000 rpm with an Ultra-Turrax T25 homogenizer (IKA, Germany). Next, this emulsion was gradually supplemented with 6 mg chitosan and 1% acetic acid with consistent homogenization at 13,000 rpm over a 3-minute period. 10 mL of Tween 20 was subsequently added to this solution, along with a small amount of the red fluorescent Rhodamine B probe, and the solution was allowed to stir in the dark for 12 h. Next, this solution was spun for 5 min at 300 rpm and diluted with PBS and ethyl acetate (1:1). Free Cur was then removed by discarding the ethyl acetate phase, while the lower phase containing the NCs was collected for downstream utilization.

RGD modification of CS/PFH-Cur-NCs was achieved via peptide cross-linking [31]. EDC-HCl (12 mg) and sulfo-NHS (12 mg) were added to the CS/PFH-Cur-NCs solution. Using NaOH, the pH was adjusted to 6.0 until the solution was clear and yellow. This mixture was then mixed constantly for 12 h at 4 °C, after which active intermediates were isolated using a Sephadex G-50 minicolumn. RGDfk was then added to the resultant solution, which was stirred continuously on ice for 24 h. A Sephadex G-50 minicolumn was then used for the purification of the prepared RGD-CS/PFH-Cur-NCs.

2.3. Nanocapsule characterization

The morphology of Cur-loaded NCs was assessed using transmission electron microscopy (TEM; JEM-2100F, JEOL, Japan). NC size, polydispersity index (PDI), and zeta potential values were measured using a Zetasizer Nano ZS90 analyzer (Malvern Instruments Ltd., Worcestershire, UK). All measurements were made in triplicate.

The structural features of chitosan, Cur, PFH, CS/PFH-Cur-NCs and RGD-CS/PFH-Cur-NCs were determined using a Thermo Scientific Nicolet iS10 Fourier transform infrared (FT-IR) spectrometer by scanning in the wavelength range of 400–4000 cm^{-1} using KBr pellets [27]. The resolution of this spectrometer was 4 cm^{-1}, and the signal-to-noise ratio was 50000:1.

Cur loading entrapment efficiency for CS/PFH-Cur-NCs and RGD-CS/PFH-Cur-NCs were calculated as follows:

$$Cur\ entrapment\ efficiency = \frac{weight\ of\ Cur\ in\ NCs}{weight\ of\ Cur\ added} \times 100\%$$

$$Cur\ loading = \frac{weight\ of\ Cur\ in\ NCs}{weight\ of\ NCs} \times 100\%$$

HPLC was used to measure free and encapsulated Cur. NCs were dissolved using ethyl acetate for these analyses, after which the solutions were spun for 2 h at 4 °C. Supernatants were then processed via HPLC to measure Cur levels in triplicate samples.

2.4. Cur loading stability analyses

The stability of free and NC-loaded Cur was evaluated by adding equivalent Cur doses of free Cur, CS/PFH-Cur-NCs, and RGD-CS/PFH-Cur-NCs to PBS (pH 7.2) and incubating these samples at 37 °C with gentle agitation. Cur concentrations remaining at specified time intervals in triplicate samples were then assessed using a UV-1900i spectrophotometer (Shimadzu Corp., Japan) ($\lambda = 424$ nm). The measurements were made in triplicate.

2.5. Ultrasound-mediated drug release assays

In order to determine the effects of 1-MHz ultrasound exposure on the release of Cur from prepared NCs, the NC solution was immersed in a plexiglas scaffold, and placed in a water bath at 37 °C. Subsequently, the NC solution was sonicated at 2 W/cm² using a 1 MHz ultrasound therapy instrument (Chattanooga Group, USA) for various specified lengths of time (0.5, 1, 2, 4, and 7 min). After sonication, the NC solution was centrifuged at 11,000 rpm, and then the Cur concentration was measured as mentioned earlier. All measurements were conducted in triplicate.

2.6. In vitro *analysis of the utility of NCs as ultrasound contrast agents*

In order to evaluate the ultrasound imaging capabilities of prepared NCs, an in vitro ultrasound imaging experiment was performed, and 1 mL of NCs was added to Latex Gloves in a custom-made trough. A GE Logic E9 instrument was then used with the following settings: 9.0 MHz center frequency, 0.13 mechanical index, and 60 dB dynamic range. For each sample, three images were taken. The Image J software was then used to analyze the gray scale values for each sample [32]. Circular regions of interest (ROIs) were outlined in each sample. All experiments were performed in triplicate.

2.7. Assessment of NC cell targetingability

MDA-MB-231 cells were plated in 24-well plates (8×10^3/well) for 24 h, following which fresh DMEM medium supplemented with Rhodamine B-labeled NCs was added to each well. The plates were then incubated for 1 h using a Constant Temperature Oscillator (Jiecheng Testing Instruments Co. Shanghai). The cells were then washed thrice with PBS to remove free NCs. The ability of CS/PFH-Cur-NCs and RGD-CS/PFH-Cur-NCs to target and bind MDA-MB-231 cells was subsequently assessed via confocal laser scanning microscopy (CLSM; Nikon A1, Nikon, USA).

2.8. Cytotoxicity assay

An MTT assay was employed to evaluate the ability of free Cur, CS/PFH-Cur-NCs, and RGD-CS/PFH-Cur-NCs to cause cytotoxic MDA-MB231 cell death. To describe briefly, cells were plated in 96-well plates (1×10^4/well) and incubated for 24 h at 37 °C in a 5% CO_2 incubator. Media was then removed, and a range of concentrations of free Cur or Cur-loaded NCs were added per well (0–60 μg/mL), with

equivalent Cur doses in each. Cells were treated for 24 h with these solutions, following which the supernatants were removed and MTT solution (10 μL; 5 mg/mL) was added to each well for an additional 4 h at 37 °C. Plates were then spun down, and 100 μL of DMSO was added per well to dissolve formazan crystals. Absorbance at 570 nm was immediately assessed via Multiskan FC Microplate Reader (Thermo Scientific, USA). Viability and IC_{50} values were then quantified, with experiments being repeated thrice.

2.9. Statistical analysis

Data were presented as means ± SD, and were analyzed via one-way ANOVAs using SPSS v22.0 (SPSS Inc., IL, USA). All statistical tests were two-tailed, and $P < 0.05$ was the significance threshold.

3. Results

3.1. Nanocapsule characterization

When assessed via TEM, prepared NCs were smooth, relatively uniform, and spheroid in shape (Figure 1). Typical NC size and zeta potential distributions have been shown in Figure 2. CS/PFH-Cur-NCs size, PDI, and zeta potential values were 458.67 ± 98.96 nm, 0.26 ± 0.04, and +15.20 ± 0.44 mV, respectively, while these values were found to be 531.20 ± 68.97 nm, 0.27 ± 0.03, and +19.20 ± 1.08 mV, respectively for RGD-CS/PFH-Cur-NCs (Figure 1).

CS/PFH-Cur-NCs entrapment efficiency and Cur loading values were 72.19 ± 2.85% and 9.62 ± 0.36%, respectively, while for RGD-CS/PFH-Cur-NCs, the corresponding values were 70.25 ± 2.56% and 9.31 ± 0.33%, respectively.

FTIR analyses were performed to determine the primary interactions involved in the formation of RGD-CS/PFH-Cur-NCs. FTIR spectra of chitosan, curcumin, PFH, CS/PFH-Cur-NCs and RGD-CS/PFH-Cur-NCs are shown in Figure 3. The ν (C–O–C), ν (NH$_2$), δ (CH$_2$OH), ν (C=O-Amide I band), and ν_{as} (CH$_2$OH) groups of chitosan exhibited respective absorption peaks at 1093 cm^{-1}, 1384 cm^{-1}, 1419 cm^{-1}, 1635 cm^{-1}, and 2923 cm^{-1}, while the –OH group was associated with a broad peak in the 3500-3000 cm^{-1} range. The Cur FTIR spectrum exhibited the characteristic peaks at 1150 cm^{-1}, 1242 cm^{-1}, and 1631 cm^{-1} attributable to ν (C–O–C), enol ν (C–O), and ν (C=C) groups. The peak at 3442 cm^{-1}

corresponded to ν (O–H). The FTIR spectra of CS/PFH-Cur-NCs and RGD-CS/PFH-Cur-NCs exhibited characteristic peaks of Cur that have largely overlapped or merged with chitosan peaks. The Cur transmission peak at around 1242 cm^{-1} was observed in the spectra of these NCs, confirming the existence of Cur in these samples. The ν (C–N), δ (C–C–N), δ (O–H), ν (C=O-Amide II band), and ν_{as} (CH$_2$) groups of RGD exhibited respective absorption peaks at 1065 cm^{-1}, 1238 cm^{-1}, 1466 cm^{-1}, 1631 cm^{-1}, and 2925 cm^{-1}, that were present in the spectrum of RGD-CS/PFH-Cur-NCs confirming the presence of RGD in these NCs.

3.2. Cur-loaded nanocapsule stability

Subsequently, the stability of Cur-loaded NCs in PBS was assessed (Figure 4), and it was found that nanocomposite Cur was relatively stable (Cur in CS/PFH-Cur-NCs > 70% and Cur in RGD-CS/PFH-Cur-NCs > 80%) over a 24 h period, whereas free Cur lost stability fairly rapidly (>80% degraded) in this same period.

3.3. Ultrasound-mediated drug release

When the prepared NCs were incubated at 37 °C without ultrasound irradiation, almost no Cur was released from these NCs within 7 min. However, sonication triggered the release of 71.4% of Cur from CS/PFH-Cur-NCs and 77.7% of Cur from RGD-CS/PFH-Cur-NCs within 4 min (Figure 5).

3.4. In vitro ultrasound imaging

The ultrasound enhancement ability of the prepared NCs was additionally evaluated *in vitro*. The NCs exhibited good enhancement ability when employed for ultrasound scanning (Figure 6), with no significant differences between RGD-CS/PFH-Cur-NCs and CS/PFH-Cur-NCs ($p = 0.578$) (Figure 6C).

3.5. Assessment of NC targeting to tumor cells

During preparation, NCs were pre-labeled with red fluorescent Rhodamine B, after which a CLSM approach was utilized for evaluating NC targeting to MDA-MB-231 cells. As shown in Figure 7, many red fluorescent NCs were evident in RGD-CS/PFH-Cur–NC–treated cells, whereas quite a few were visible in CS/PFH-Cur–NC–treated cells.

CS/PFH-Cur   RGD-CS/PFH-Cur

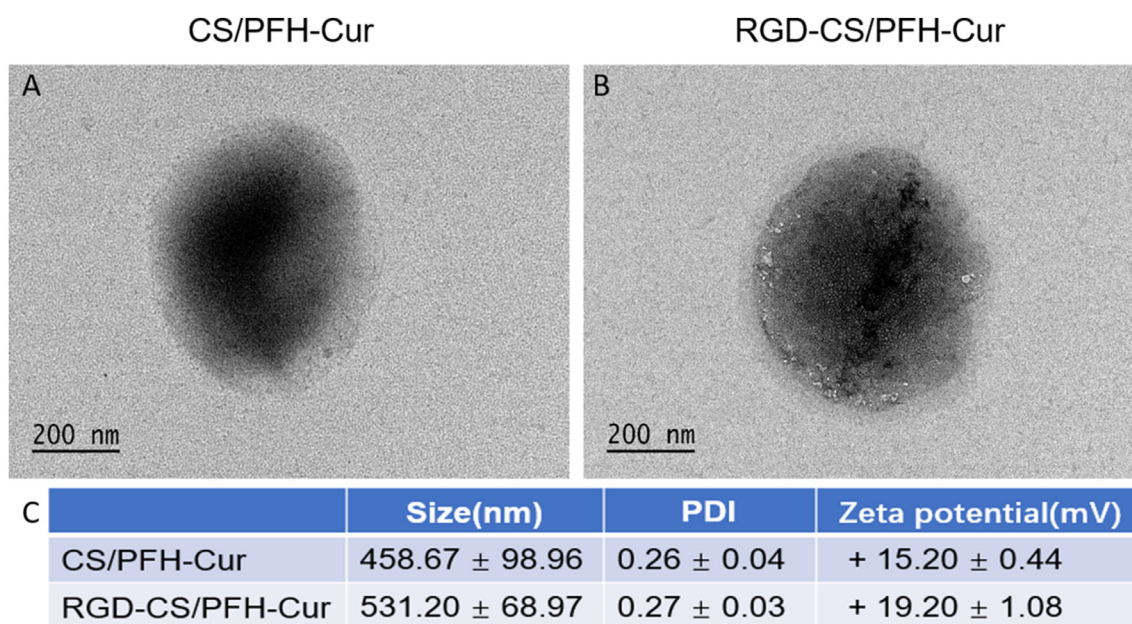| C	Size(nm)	PDI	Zeta potential(mV)
CS/PFH-Cur	458.67 ± 98.96	0.26 ± 0.04	+ 15.20 ± 0.44
RGD-CS/PFH-Cur	531.20 ± 68.97	0.27 ± 0.03	+ 19.20 ± 1.08

Figure 1. Morphology and structure of CS/PFH-Cur-NC (A) and RGD-CS/PFH-Cur-NC (B). Nanocapsules assess via TEM (the scale bar represents 200 nm) (C) Size, PDI, and zeta potential values of CS/PFH-Cur-NCs and RGD-CS/PFH-Cur-NCs.
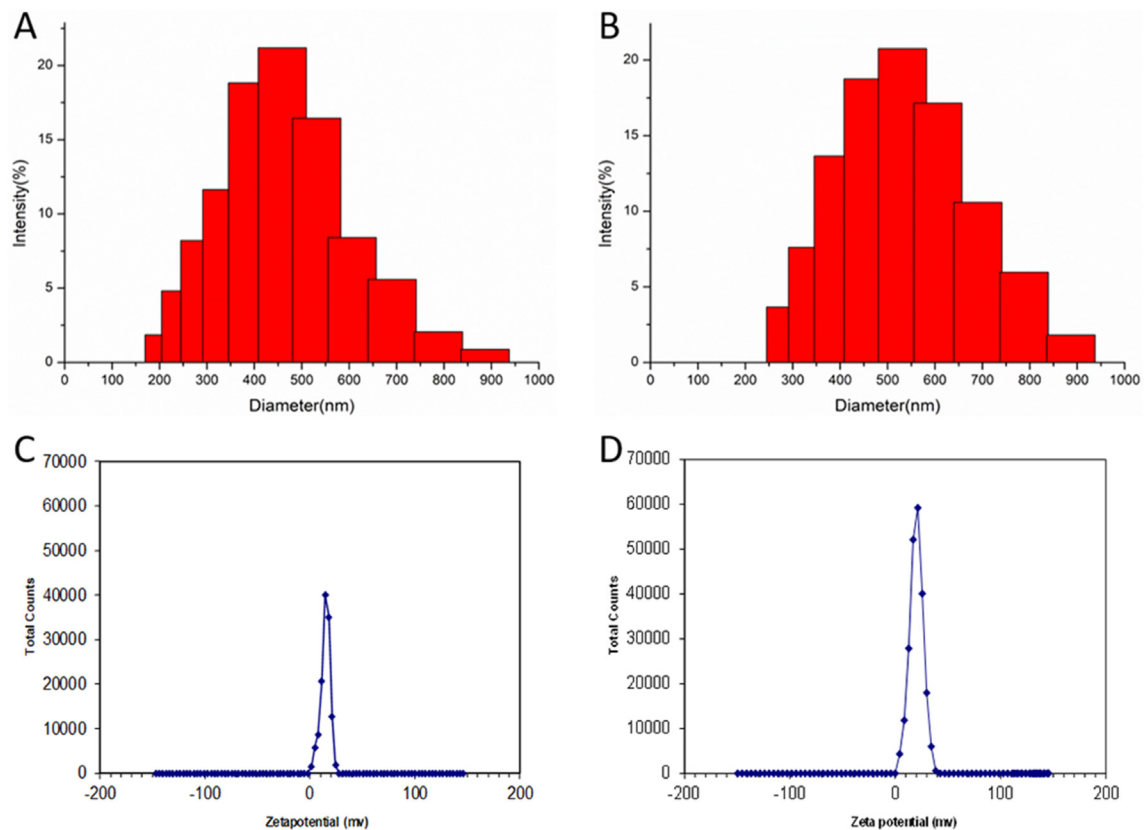
Figure 2. The sizes and zeta potential distributions of CS/PFH-Cur-NCs (A,C) and RGD-CS/PFH-Cur-NCs (B,D).
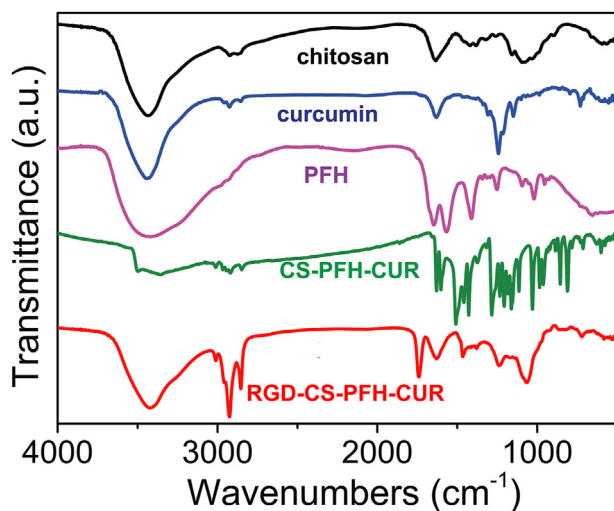

Figure 3. FTIR spectra of chitosan, curcumin, PFH, CS/PFH-Cur-NCs and RGD-CS/PFH-Cur-NCs.
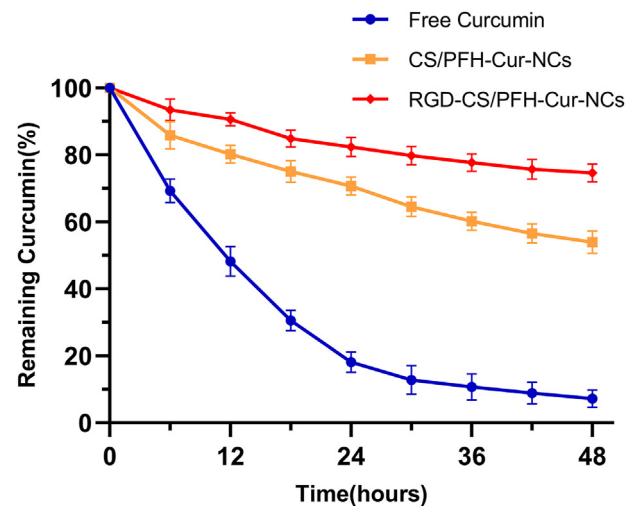

Figure 4. Curcumin stability. Stability of free curcumin, CS/PFH-Cur-NCs, and RGD-CS/PFH-Cur-NCs in PBS (pH 7.2). Means $\pm$ SD (n = 3).

3.6. Cytotoxicity assay

Lastly, we employed an MTT assay to assess the relative cytotoxicity of free Cur and Cur-loaded NCs by treating MDA-MB-231 cells for 24 h with a range of concentrations (0–60 μg/mL) of the corresponding preparations. By utilizing this approach, the IC_{50} values of free Cur, CS/PFH-Cur-NCs, and RGD-CS/PFH-Cur-NCs were determined to be 26.23 ± 2.76, 15.95 ± 1.57, and 10.65 ± 0.97 μg/mL, respectively at 24 h (Figure 8). There were significant differences among these three groups ($P < 0.05$).

4. Discussion

With the advances in nanotechnology research, many different NC formulations have been designed and investigated in the fields of targeted molecular imaging and tumor treatment [33]. Chitosan is a natural biopolymer that is produced following the deacetylation of chitin [34], which is widely found in the shells of crustaceans including shrimp and crabs [35]. Chitosan offers a variety of promising biological activities, while also manifesting excellent biocompatibility and biodegradability [36]. Owing to these promisingcharacteristics, chitosan is often used as an excipient in various drug delivery applications [37, 38, 39], with
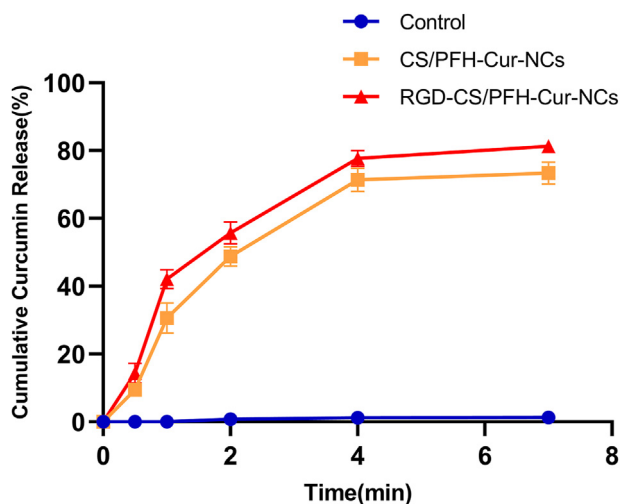
Figure 5. *In vitro* release profiles of curcumin from nanocapsules (CS/PFH-Cur-NCs and RGD-CS/PFH-Cur-NCs) with sonication and without sonication (control) in pH 7.4, means ± SD (n = 3).

chitosan-based preparations being capable of targeted, controlled drug delivery, with the capacity to accomplish gradual release of drugs. Such chitosan-based approaches can significantly enhance the key pharmacodynamic parameters of drugs including drug absorption and bioavailability while reducing toxicity and associated adverse side effects. NCs are retained within tumor tissues due to the enhanced permeability and retention effect (EPR), however, this property alone is generally not thought to be sufficient to achieve reliable and robust tumor targeting [40]. RGD peptides, however, can effectively enhance NC penetration into tumor tissues that express high levels of the integrin αvβ3 [41,42], thereby enhancing the therapeutic efficacy of these preparations. In this study we were able to successfully prepare novel RGD-modified Cur-loaded CS/PFH NCs via nano-emulsification, resulting in the formation of uniformly distributed and well-dispersed

particles. These RGD-modified NCs combine the utility of the EPR effect with RGD-mediated tumor selectivity to bolster anti-tumor drug efficacy while simultaneously reducing the incidence and severity of off-target toxicity.

It was found that Cur incorporated within our prepared NCs was relatively stable over a 24 period (CS/PFH-Cur-NCs > 60% and RGD-CS/PFH-Cur-NCs > 80%), whereas over 80% of free Cur molecules were degraded within the same duration. This suggests that Cur encapsulation within chitosan-based NCs can significantly enhance its stability in aqueous solutions.

Almost no Cur was released from NCs for 7-minute in the absence of sonication, thereby suggesting that the NC shell was conducive to robust drug retention. However, rapid Cur release occurred within the first few minutes of ultrasonic irradiation, with subsequent slow drug release, however, continuing with further sonication.

As the RGD peptide specifically and readily binds to the αvβ3 integrin, MDA-MB-231 cells that express high levels of the αvβ3 integrin were selected for analyses of RGD-CS/PFH-Cur-NCs. It was found that these RGD-modified NCs were able to target MDA-MB-231 cells more readily and were internalized by these cells, which corroborates well with the prior results [43]. More importantly, this internalization was superior to that observed for unmodified NCs, suggesting that RGD was able to specifically bind to αvβ3 integrin occurring on the cell surface to facilitate the targeted uptake of these NCs into tumor cells.

We additionally employed an MTT assay approach to examine the ability of these NCs to induce cytotoxic MDA-MB-231 cell death. It was found that cytotoxicity was dose-dependent in all samples and increased with increasing Cur dose. Our results further revealed that encapsulating Cur into CS/PFH NCs can enhance its cytotoxicity and lower the associated IC_{50} values owing to the enhanced stability and prolonged release of Cur, thereby facilitating enhanced cancer celldeath. It was also found that free Cur has a lower ability kill cancer cells than CS/PFH-Cur-NCs or RGD-CS/PFH-Cur-NCs. This may be ascribed to the poor stability and limited cellular uptake of free Cur. In addition, as Cur is highly lipophilic it may be incorporated into cell membranes, thereby restricting it from diffusing within. In contrast, Cur-loaded NCs can be internalized via endocytosis. The differences in cytotoxicity for these two types of NC
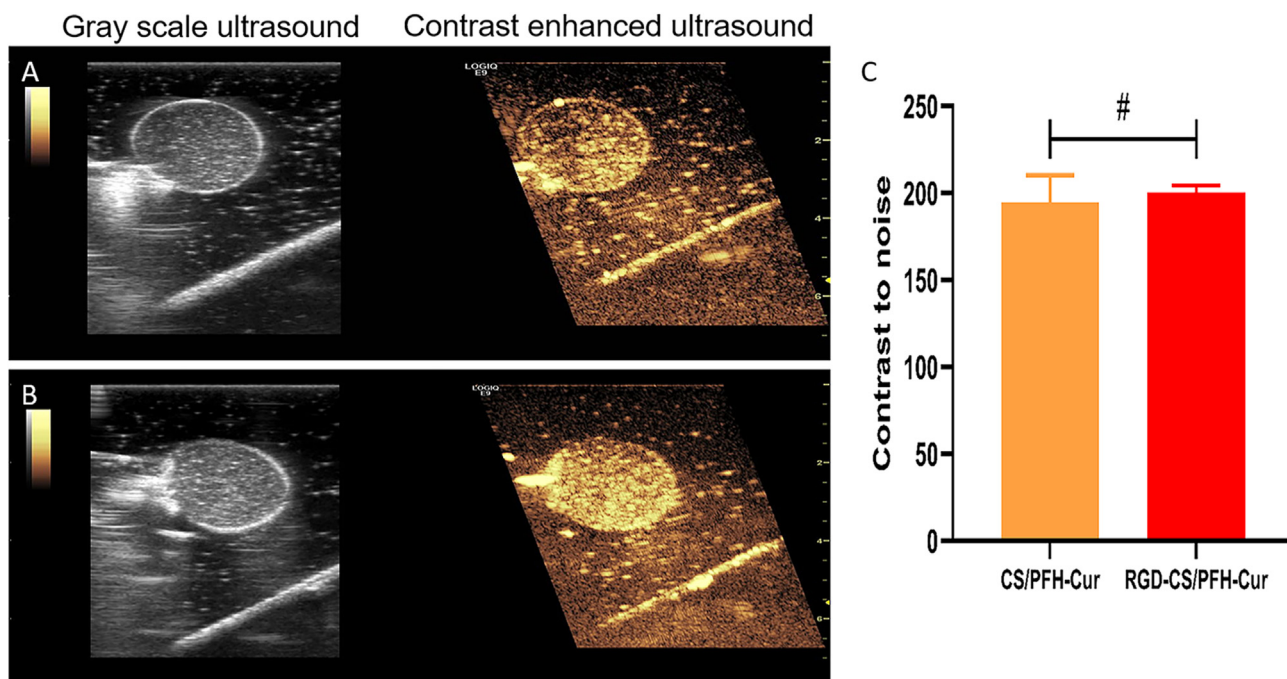

Figure 6. *In vitro* ultrasound enhancement image. Ultrasound images of CS/PFH-Cur-NCs (A) and RGD-CS/PFH-Cur-NCs (B) using a 9.0 MHz probe (C) There was no significant difference of the enhancement ability between two kinds of nanocapsules (#P > 0.05).
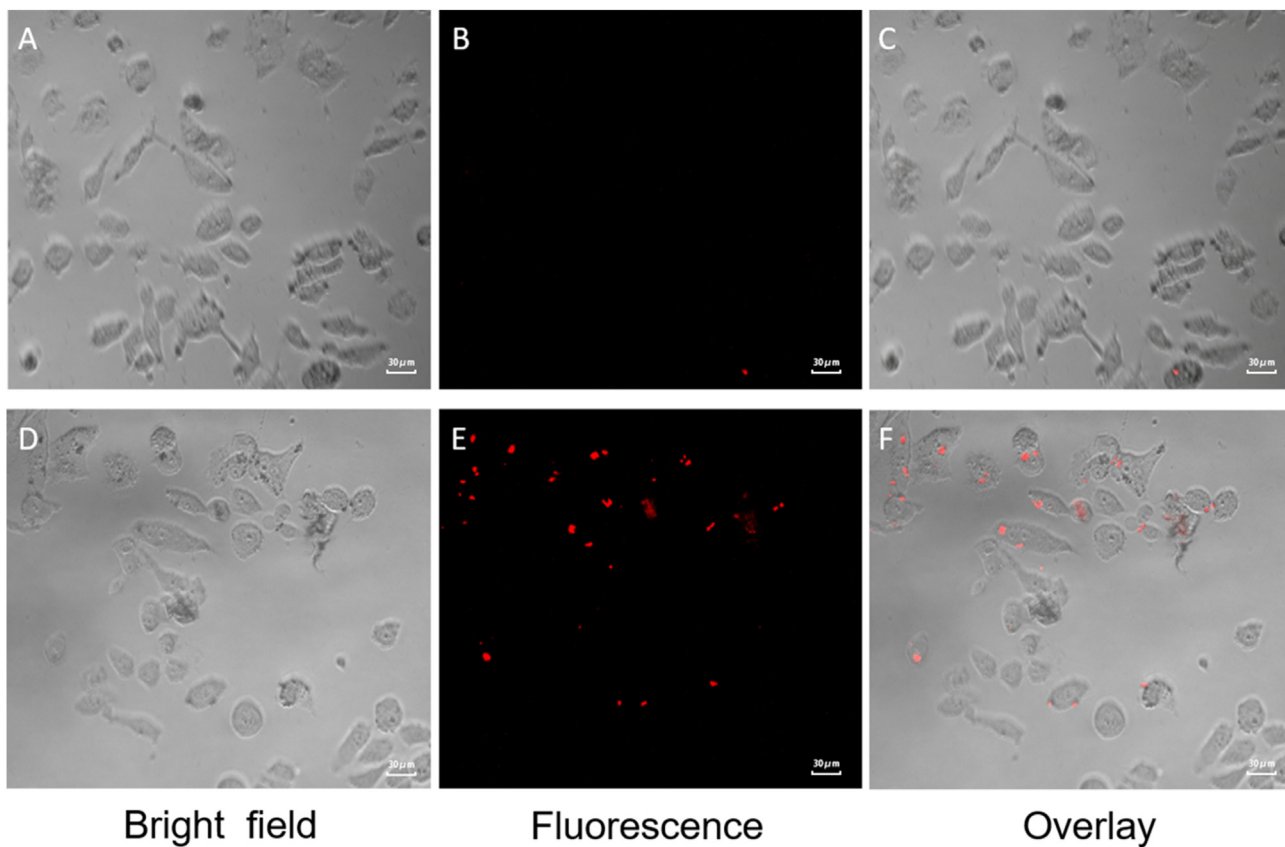
Figure 7. The cell-targeting capabilities of NCs were assessed *in vitro* via CLSM (A–C) MDA-MB-231 cells treated with CS/PFH-Cur-NCs (D–F) MDA-MB-231 cells treated with RGD-CS/PFH-Cur-NCs (The scale bar represents 30 μm).
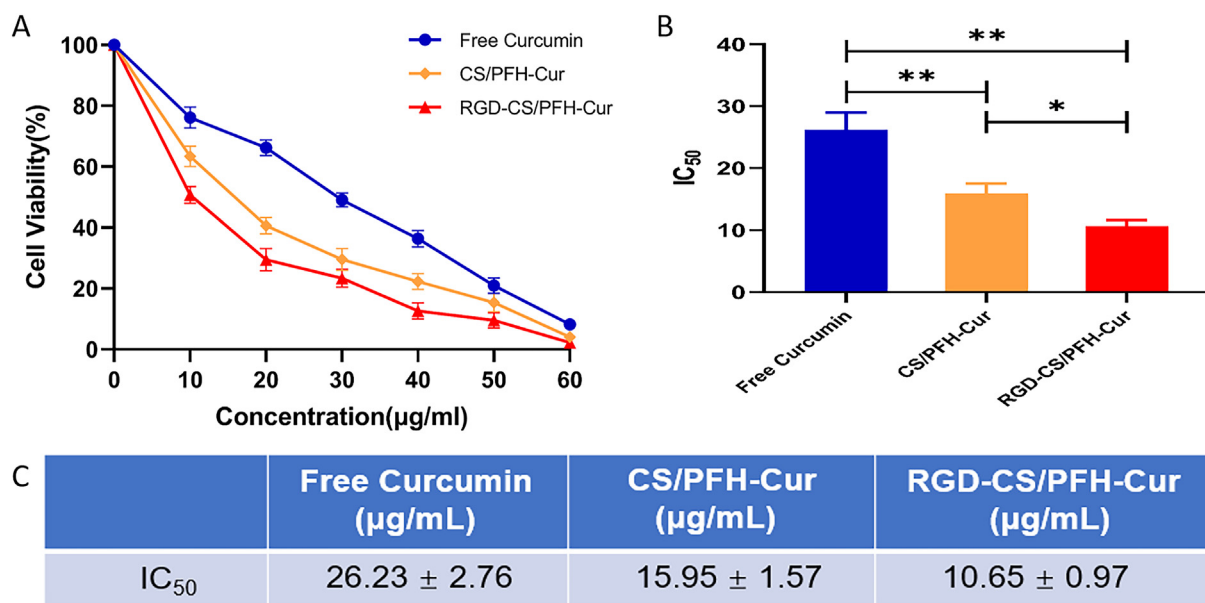

	Free Curcumin (μg/mL)	CS/PFH-Cur (μg/mL)	RGD-CS/PFH-Cur (μg/mL)
IC$_{50}$	26.23 ± 2.76	15.95 ± 1.57	10.65 ± 0.97

Figure 8. The impact of free curcumin, CS/PFH-Cur-NCs, and RGD-CS/PFH-Cur-NCs on MDA-MB-231 cell viability after a 24 h treatment. The IC$_{50}$ values of free Cur, CS/PFH-Cur-NCs, and RGD-CS/PFH-Cur-NCs were 26.23 ± 2.76, 15.95 ± 1.57, and 10.65 ± 0.97 μg/mL respectively; Means ± SD (n = 3) (*$P < 0.05$. **$P < 0.01$).

preparations could also be observed. Our results also indicate that RGD modification can enhance NC internalization into tumor cells, thereby boosting subsequent cell death.

While our results highlight the promising tumor-targeting and cytotoxic properties of our novel RGD-CS/PFH-Cur-NCs, it is important to note that these results were obtained following *in vitro* analysis. Future in-depth and *in vivo* analyses will be essential to develop a comprehensive understanding of the therapeutic utility of these and similar NC preparations in order to lay the foundation for precise and reliable drug delivery to cancer patients.

5. Conclusions

The present study comprises the successful preparation of novel RGD-modified Cur-loaded CS/PFH NCs that exhibit superior Cur delivery to tumor cells relative to CS/PFH-Cur-NCs or free Cur, thereby suggesting that these RGD-CS/PFH-Cur-NCs may be an ideal approach for improving the therapeutic administration of Cur. As such, these and similar nano-capsular drug delivery strategies have promising potential in the field of targeted cancer therapy and call for extensive further investigations.

Declarations

Author contribution statement

Liang Wang: Conceived and designed the experiments; Performed the experiments; Contributed reagents, materials, analysis tools or data; Wrote the paper.

Shixia Zhu, Chunpeng Zou, Hongju Kou, Maosheng Xu: Performed the experiments; Analyzed and interpreted the data; Contributed reagents, materials, analysis tools or data.

Jie Li: Conceived and designed the experiments; Contributed reagents, materials, analysis tools or data.

Data availability statement

Data will be made available on request.

Declaration of interest's statement

The authors declare no conflict of interest.

Additional information

No additional information is available for this paper.

References

[1] P. Baharuddin, N. Satar, K.S. Fakiruddin, N. Zakaria, M.N. Lim, N.M. Yusoff, Z. Zakaria, B.H. Yahaya, Curcumin improves the efficacy of cisplatin by targeting cancer stem-like cells through p21 and cyclin D1-mediated tumour cell inhibition in non-small cell lung cancer cell lines, Oncol. Rep. 35 (1) (2016) 13–25.

[2] H. Abbas, Y.A. El-Feky, M.M. Al-Sawahli, N.M. El-Deeb, H.B. El-Nassan, M. Zewail, Development and optimization of curcumin analog nano-bilosomes using 2(1).3(1) full factorial design for anti-tumor profiles improvement in human hepatocellular carcinoma: in-vitro evaluation, in-vivo safety assay, Drug Deliv. 29 (1) (2022) 714–727.

[3] M. Hatamipour, F. Hadizadeh, M.R. Jaafari, Z. Khashyarmanesh, T. Sathyapalan, A. Sahebkar, Anti-proliferative potential of fluorinated curcumin analogues: experimental and computational analysis and review of the literature, Curr. Med. Chem. 29 (8) (2022) 1459–1471.

[4] F. Jahanbakhshi, P. Maleki Dana, B. Badehnoosh, B. Yousefi, M.A. Mansournia, M. Jahanshahi, Z. Asemi, J. Halajzadeh, Curcumin anti-tumor effects on endometrial cancer with focus on its molecular targets, Cancer Cell Int. 21 (1) (2021) 120.

[5] K.V. Kavya, S. Vargheese, S. Shukla, I. Khan, D.K. Dey, V.K. Bajpai, K. Thangavelu, R. Vivek, R.T.R. Kumar, Y.K. Han, Y.S. Huh, Y. Haldorai, A cationic amino acid polymer nanocarrier synthesized in supercritical CO2 for co-delivery of drug and gene to cervical cancer cells, Colloids Surf. B Biointerfaces 216 (2022), 112584.

[6] Y. Peng, M. Ao, B. Dong, Y. Jiang, L. Yu, Z. Chen, C. Hu, R. Xu, Anti-inflammatory effects of curcumin in the inflammatory diseases: status, limitations and countermeasures, Drug Des. Dev. Ther. 15 (2021) 4503–4525.

[7] C.A. Mohammad, K.M. Ali, A.M. Sha, S.S. Gul, Antioxidant effects of curcumin gel in experimental induced diabetes and periodontitis in rats, BioMed Res. Int. 2022 (2022) 7278064.

[8] A. Shakeri, M.R. Zirak, A. Wallace Hayes, R. Reiter, G. Karimi, Curcumin and its analogues protect from endoplasmic reticulum stress: mechanisms and pathways, Pharmacol. Res. 146 (2019) 104335.

[9] H. Celik, T. Aydin, K. Solak, S. Khalid, A.A. Farooqi, Curcumin on the "flying carpets" to modulate different signal transduction cascades in cancers: next-generation approach to bridge translational gaps, J. Cell. Biochem. 119 (6) (2018) 4293–4303.

[10] L.D. Liu, Y.X. Pang, X.R. Zhao, R. Li, C.J. Jin, J. Xue, R.Y. Dong, P.S. Liu, Curcumin induces apoptotic cell death and protective autophagy by inhibiting AKT/mTOR/p70S6K pathway in human ovarian cancer cells, Arch. Gynecol. Obstet. 299 (6) (2019) 1627–1639.

[11] A.Q. Khan, E.I. Ahmed, N. Elareer, H. Fathima, K.S. Prabhu, K.S. Siveen, M. Kulinski, F. Azizi, S. Dermime, A. Ahmad, M. Steinhoff, S. Uddin, Curcumin-mediated apoptotic cell death in papillary thyroid cancer and cancer stem-like cells through targeting of the JAK/STAT3 signaling pathway, Int. J. Mol. Sci. 21 (2) (2020).

[12] F. Ravindran, J. Koroth, M. Manjunath, S. Narayan, B. Choudhary, Curcumin derivative ST09 modulates the miR-199a-5p/DDR1 axis and regulates proliferation and migration in ovarian cancer cells, Sci. Rep. 11 (1) (2021) 23025.

[13] T. Yaguchi, Y. Kawakami, Cancer-induced heterogeneous immunosuppressive tumor microenvironments and their personalized modulation, Int. Immunol. 28 (8) (2016) 393–399.

[14] H. Mirzaei, H. Bagheri, F. Ghasemi, J.M. Khoi, M.H. Pourhanifeh, Y.V. Heyden, E. Mortezapour, A. Nikdasti, P. Jeandet, H. Khan, A. Sahebkar, Anti-cancer activity of curcumin on multiple myeloma, Anti Cancer Agents Med. Chem. 21 (5) (2021) 575–586.

[15] R.R. Kotha, D.L. Luthria, Curcumin: biological, pharmaceutical, nutraceutical, and analytical aspects, Molecules 24 (16) (2019).

[16] A. Berry, B. Collacchi, R. Masella, R. Vari, F. Cirulli, Curcuma longa, the "golden spice" to counteract neuroinflammaging and cognitive decline-what have we learned and what needs to Be done, Nutrients 13 (5) (2021).

[17] B. Salehi, C.F. Rodrigues, G. Peron, S. Dall'Acqua, J. Sharifi-Rad, I. Azmi, I. Shukla, U. Singh Baghel, A. Prakash Mishra, A.M. Elissawy, A.N. Singab, R. Pezzani, M. Redaelli, J.K. Patra, C. Kulandaisamy Venil, G. Das, D. Singh, P. Kriplani, A. Venditti, P.V.T. Fokou, M. Iriti, R. Amarowicz, M. Martorell, N. Cruz-Martins, Curcumin nanoformulations for antimicrobial and wound healing purposes, Phytother Res. (2021).

[18] R. Klippstein, J.T. Wang, R.I. El-Gogary, J. Bai, F. Mustafa, N. Rubio, S. Bansal, W.T. Al-Jamal, K.T. Al-Jamal, Passively targeted curcumin-loaded PEGylated PLGA nanocapsules for colon cancer therapy in vivo, Small 11 (36) (2015) 4704–4722.

[19] L. Lugasi, I. Grinberg, R. Sabag, R. Madar, H. Einat, S. Margel, Proteinoid nanocapsules as drug delivery system for improving antipsychotic activity of risperidone, Molecules 25 (17) (2020).

[20] R.P. Moura, C. Pacheco, A.P. Pego, A. des Rieux, B. Sarmento, Lipid nanocapsules to enhance drug bioavailability to the central nervous system, J. Contr. Release 322 (2020) 390–400.

[21] C. Di Cicco, R. Vecchione, V. Quagliariello, A. Busato, I. Tufano, E. Bedini, M. Gerosa, A. Sbarbati, F. Boschi, P. Marzola, N. Maurea, P.A. Netti, Biocompatible, photo-responsive layer-by-layer polymer nanocapsules with an oil core: in vitro and in vivo study, J. R. Soc. Interface 19 (187) (2022), 20210800.

[22] V.K. Bajpai, S. Shukla, S.M. Kang, S.K. Hwang, X. Song, Y.S. Huh, Y.K. Han, Developments of cyanobacteria for nano-marine drugs: relevance of nanoformulations in cancer therapies, Mar. Drugs 16 (6) (2018).

[23] J.B. Vines, J.H. Yoon, N.E. Ryu, D.J. Lim, H. Park, Gold nanoparticles for photothermal cancer therapy, Front. Chem. 7 (2019) 167.

[24] J. Zhang, N. Lu, L. Weng, Z. Feng, J. Tao, X. Su, R. Yu, W. Shi, Q. Qiu, Z. Teng, L. Wang, General and facile syntheses of hybridized deformable hollow mesoporous organosilica nanocapsules for drug delivery, J. Colloid Interface Sci. 583 (2021) 714–721.

[25] S. Ranjbar, Y. Fatahi, F. Atyabi, The quest for a better fight: how can nanomaterials address the current therapeutic and diagnostic obstacles in the fight against COVID-19? J. Drug Deliv. Sci. Technol. 67 (2022) 102899.

[26] Q. Hu, Y. Luo, Chitosan-based nanocarriers for encapsulation and delivery of curcumin: a review, Int. J. Biol. Macromol. 179 (2021) 125–135.

[27] F. Baghbani, M. Chegeni, F. Moztarzadeh, S. Hadian-Ghazvini, M. Raz, Novel ultrasound-responsive chitosan/perfluorohexane nanodroplets for image-guided smart delivery of an anticancer agent: Curcumin, Mater Sci Eng C Mater Biol Appl 74 (2017) 186–193.

[28] E. Bari, M. Serra, M. Paolillo, E. Bernardi, S. Tengattini, F. Piccinini, C. Lanni, M. Sorlini, G. Bisbano, E. Calleri, M.L. Torre, S. Perteghella, Silk fibroin nanoparticle functionalization with arg-gly-asp cyclopentapeptide promotes active targeting for tumor site-specific delivery, Cancers 13 (5) (2021).

[29] X. Xia, X. Yang, P. Huang, D. Yan, ROS-responsive nanoparticles formed from RGD-epothilone B conjugate for targeted cancer therapy, ACS Appl. Mater. Interfaces 12 (16) (2020) 18301–18308.

[30] A. Ouyang, D. Zhao, X. Wang, W. Zhang, T. Jiang, A. Li, W. Liu, Covalent RGD-graphene-phthalocyanine nanocomposite for fluorescence imaging-guided dual active/passive tumor-targeted combinatorial phototherapy, J. Mater. Chem. B 10 (2) (2022) 306–320.

[31] J. Xu, J.H. Zhao, Y. Liu, N.P. Feng, Y.T. Zhang, RGD-modified poly(D,L-lactic acid) nanoparticles enhance tumor targeting of oridonin, Int. J. Nanomed. 7 (2012) 211–219.

[32] S. Duan, L. Guo, D. Shi, M. Shang, D. Meng, J. Li, Development of a novel folate-modified nanobubbles with improved targeting ability to tumor cells, Ultrason. Sonochem. 37 (2017) 235–243.

[33] H.Y. Huang, S.H. Hu, S.Y. Hung, C.S. Chiang, H.L. Liu, T.L. Chiu, H.Y. Lai, Y.Y. Chen, S.Y. Chen, SPIO nanoparticle-stabilized PAA-F127 thermosensitive nanobubbles with MR/US dual-modality imaging and HIFU-triggered drug release for magnetically guided in vivo tumor therapy, J. Contr. Release 172 (1) (2013) 118–127.

[34] M.K. Nguyen, E. Alsberg, Bioactive factor delivery strategies from engineered polymer hydrogels for therapeutic medicine, Prog. Polym. Sci. 39 (7) (2014) 1236–1265.

[35] C.L. Luchese, J.M.F. Pavoni, N.Z. Dos Santos, L.K. Quines, L.D. Pollo, J.C. Spada, I.C. Tessaro, Effect of chitosan addition on the properties of films prepared with corn and cassava starches, J. Food Sci. Technol. 55 (8) (2018) 2963–2973.

[36] D. Wei, Q. Liu, Z. Liu, J. Liu, X. Zheng, Y. Pei, K. Tang, Modified nano microfibrillated cellulose/carboxymethyl chitosan composite hydrogel with giant network structure and quick gelation formability, Int. J. Biol. Macromol. 135 (2019) 561–568.

[37] S. Anbazhagan, K.P. Thangavelu, Application of tetracycline hydrochloride loaded-fungal chitosan and Aloe vera extract based composite sponges for wound dressing, J. Adv. Res. 14 (2018) 63–71.

[38] Y. Tian, P. Deng, Y. Wu, Z. Ding, G. Li, J. Liu, Q. He, A simple and efficient molecularly imprinted electrochemical sensor for the selective determination of tryptophan, Biomolecules 9 (7) (2019).

[39] M.A. Tomeh, R. Hadianamrei, X. Zhao, A review of curcumin and its derivatives as anticancer agents, Int. J. Mol. Sci. 20 (5) (2019).

[40] P.E. Saw, S. Jon, Understanding of the Entry Mechanism of Nanoparticles into Tumors Determines the Future Direction of Nanomedicine Development, BIO Integration 1, 2020, pp. 193–195.

[41] K.N. Sugahara, T. Teesalu, P.P. Karmali, V.R. Kotamraju, L. Agemy, D.R. Greenwald, E. Ruoslahti, Coadministration of a tumor-penetrating peptide enhances the efficacy of cancer drugs, Science 328 (5981) (2010) 1031–1035.

[42] D. Kebebe, Y. Wu, B. Zhang, J. Yang, Y. Liu, X. Li, Z. Ma, P. Lu, Z. Liu, J. Li, Dimeric c(RGD) peptide conjugated nanostructured lipid carriers for efficient delivery of Gambogic acid to breast cancer, Int. J. Nanomed. 14 (2019) 6179–6195.

[43] C. Yang, J. Uertz, D.B. Chithrani, Colloidal gold-mediated delivery of bleomycin for improved outcome in chemotherapy, Nanomaterials (Basel) 6 (3) (2016).